

# Supplemental: A Multi-Scale Model for Simulating Liquid-Hair Interactions

YUN (RAYMOND) FEI and HENRIQUE TELES MAIA, Columbia University

CHRISTOPHER BATTY, University of Waterloo

CHANGXI ZHENG and EITAN GRINSPUN, Columbia University

## ACM Reference format:

Yun (Raymond) Fei, Henrique Teles Maia, Christopher Batty, Changxi Zheng, and Eitan Grinspun. 2017. Supplemental: A Multi-Scale Model for Simulating Liquid-Hair Interactions. *ACM Trans. Graph.* 36, 4, Article 56 (July 2017), 5 pages.

<https://doi.org/http://dx.doi.org/10.1145/3072959.3073630>

## S1 SURFACE POTENTIAL OF WET HAIR

We can derive the surface potential energy used for the cohesion force in the main paper as follows. Given the surface tension coefficient between the liquid-air interface  $\sigma_{LA}$ , the solid-air interface  $\sigma_{SA}$ , and the liquid-solid interface  $\sigma_{LS}$ , the surface tension energy is the surface area times the corresponding coefficients

$$dE_s = [\sigma_{LA}l_{LA}(s) + \sigma_{SA}l_{SA}(s) + \sigma_{LS}l_{LS}(s)] ds, \quad (S1)$$

Applying the Young's equation (Young 1805),

$$\sigma_{SA} - \sigma_{LS} - \sigma_{LA}\cos\theta = 0 \quad (S2)$$

where  $\theta$  is the equilibrium contact angle, we have

$$dE_s = [\sigma_{LA}(l_{LA}(s) + l_{SA}(s)\cos\theta) + \sigma_{LS}(l_{SA}(s) + l_{LS}(s))] ds. \quad (S3)$$

The sum of the length of the solid-air and liquid-solid interfaces is exactly the length of the solid interface, which is a constant value and does not affect the potential gradient. For our purpose we can simply set  $\sigma_{LS} = 0$ . Hence we have

$$dE_s = [\sigma_{LA}(l_{LA}(s) + l_{SA}(s)\cos\theta)] ds, \quad (S4)$$

which matches the form given in the paper, up to minor notational changes.

## S2 REDUCED LIQUID MODEL ON HAIR

The derivation for our 1D reduced-liquid model generally follows the strategy used for the classical shallow water equation (Barré de Saint-Venant 1871), with differences that account for the cylindrical geometry. We first parameterize the variables on the tangential direction of a hair segment.

$$u = u(x), h = h(x), A_L = A_L(x) \quad (S5)$$

where  $u$  is the velocity in the frame of a hair segment, and  $A_L$  is the area of the cross section.

© 2017 Copyright held by the owner/author(s). Publication rights licensed to Association for Computing Machinery.

This is the author's version of the work. It is posted here for your personal use. Not for redistribution. The definitive Version of Record was published in *ACM Transactions on Graphics*, <https://doi.org/http://dx.doi.org/10.1145/3072959.3073630>.

Consider the mass flux passing through a point on the hair segment. For a point  $x$  the mass flux is  $\rho A_L(x)u(x)\delta t$ , and the flux passing through its neighbor coordinate  $x + dx$  is  $\rho A_L(x + dx)u(x + dx)\delta t$ . Hence we have

$$dm = \rho A_L(x)u(x)\delta t - \rho A_L(x + dx)u(x + dx)\delta t \quad (S6)$$

$$\frac{dm}{dt} = -\rho \frac{A_L(x + dx)u(x + dx) - A_L(x)u(x)}{dx} dx$$

Since  $dm = \rho dA_L dx$ , the factors of  $\rho dx$  cancel on both sides leaving us with

$$\frac{dA_L}{dt} = -\frac{A_L(x + dx)u(x + dx) - A_L(x)u(x)}{dx} \quad (S7)$$

Taking the limit of  $dx \rightarrow 0$  and  $dt \rightarrow 0$ , we have

$$\frac{\partial A_L}{\partial t} = -\frac{\partial(A_L u)}{\partial x} \quad (S8)$$

We also have  $A_L = \pi [(h + r)^2 - r^2]$ . Thus we have the equation of continuity for reduced liquid on cylindrical hair segments by canceling  $\pi$

$$\frac{\partial}{\partial t} [(h + r)^2] + \frac{\partial}{\partial x} [(h + r)^2 - r^2] u = 0. \quad (S9)$$

Since the hairs themselves are moving, we also need momentum conservation in 3D for the system including both hairs and liquid, and we argue that the momentum transfer equation (14) is a direct result from the momentum conservation of this Eulerian-on-Lagrangian (Fan et al. 2013) system.

As an observer following the hair velocity  $\mathbf{v}_H$ , for any variable  $v$  of the liquid on hair whose tangential direction is denoted by  $\mathbf{e}$  we have the following momentum conservation from the Navier-Stokes equation

$$\frac{\partial \mathbf{v}}{\partial t} + (u\mathbf{e}) \cdot \nabla \mathbf{v} = \left( -\frac{1}{\rho_L} \frac{\partial p}{\partial x} + a_{\text{ext}} \right) \mathbf{e} \quad (S10)$$

whose right hand side only performs in the direction of  $\mathbf{e}$ .

Here  $\mathbf{v} = u\mathbf{e} + \mathbf{v}_H$  is simply the liquid flow velocity in the 3D space. By substitution and expansion we have

$$\frac{\partial u}{\partial t} \mathbf{e} + u(\mathbf{e} \cdot \nabla u)\mathbf{e} + \frac{\partial \mathbf{v}_H}{\partial t} + u\mathbf{e} \cdot \nabla \mathbf{v}_H = \left( -\frac{1}{\rho_L} \frac{\partial p}{\partial x} + a_{\text{ext}} \right) \mathbf{e} \quad (S11)$$

Since  $\mathbf{e} \cdot \nabla$  is simply the directional derivative in  $\mathbf{e}$ , we rewrite it with the derivative in  $x$  which is

$$\frac{\partial u}{\partial t} \mathbf{e} + u \frac{\partial u}{\partial x} \mathbf{e} + \frac{\partial \mathbf{v}_H}{\partial t} + u \frac{\partial \mathbf{v}_H}{\partial x} = \left( -\frac{1}{\rho_L} \frac{\partial p}{\partial x} + a_{\text{ext}} \right) \mathbf{e} \quad (S12)$$

Since we also have the momentum conservation on hair which is  $\frac{\partial u}{\partial t} = -u \frac{\partial u}{\partial x} - \frac{1}{\rho_L} \frac{\partial p}{\partial x} + a_{\text{ext}}$ , by substitution we have

$$\frac{\partial \mathbf{v}_H}{\partial t} + u \frac{\partial \mathbf{v}_H}{\partial x} = 0 \quad (S13)$$

Next we move the liquid velocity  $u$  into the derivative. Firstly we multiply the equation with cross section area  $A_L$  and manipulate the terms as

$$A_L \frac{\partial \mathbf{v}_H}{\partial t} + \frac{\partial A_L}{\partial t} \cdot \mathbf{v}_H + A_L u \frac{\partial \mathbf{v}_H}{\partial x} - \frac{\partial A_L}{\partial t} \cdot \mathbf{v}_H = 0. \quad (\text{S14})$$

By substitution with (S8), we have

$$A_L \frac{\partial \mathbf{v}_H}{\partial t} + \frac{\partial A_L}{\partial t} \cdot \mathbf{v}_H + A_L u \frac{\partial \mathbf{v}_H}{\partial x} + \frac{\partial}{\partial x} (A_L u) \cdot \mathbf{v}_H = 0, \quad (\text{S15})$$

where the derivatives can be combined as

$$\frac{\partial}{\partial t} (A_L \mathbf{v}_H) + \frac{\partial}{\partial x} (A_L u \mathbf{v}_H) = 0. \quad (\text{S16})$$

By substitution where  $A_L = \pi [(h+r)^2 - r^2]$  we have (14)

$$\frac{\partial}{\partial t} [((h+r)^2 - r^2) \mathbf{v}_H] + \frac{\partial}{\partial x} [((h+r)^2 - r^2) u \mathbf{v}_H] = 0. \quad (\text{S17})$$

### S3 PRECOMPUTATION FOR COHESION MODEL

Since  $R(d_{ij}, A_{Lij})$  and  $\alpha_k(d_{ij}, A_{Lij})$  are implicitly defined by  $d_{ij}$  and  $A_{Lij}$ , we precompute  $\frac{\partial d E_{s,ij}}{\partial d}$  and store its values into a table for efficiency. At run-time we can interpolate from the table to get  $\frac{\partial d E_{s,ij}}{\partial d}$ .

The first step of precomputation is building the table of  $A_{Lij}(d_{ij}, \alpha_k)$  for all combinations of a uniformly sampled set of values of  $d_{ij}$  and  $\alpha_k$ , following (6). Since  $d_{ij} < d_{\max}$ , where the latter is computed with (9), the range of possible  $d_{ij}$  values is bounded.

After we have the table of  $A_L$ , we uniformly discretize the range of resulting  $A_L$  values to compute a mesh grid for  $\alpha_1$  and  $\alpha_2$ : for each sample  $(d, A_L)$  on the mesh grid, we search for the closest  $A_L$  in the table with binary search and linearly interpolate to get the inverse mapping  $\alpha(A_L, d)$ . Then we solve (7) for each sample of  $(d, A_L)$  to get  $\frac{\partial R(d, A_L)}{\partial d}$  and  $\frac{\partial \alpha(d, A_L)}{\partial d}$ .

Finally, using the derivatives of (22) and (23), we can find the gradient of (21) as

$$\nabla_d E_T(d, A_L) = \sigma \left[ \frac{\partial l_A(d, A_L)}{\partial d} + \sum_{k=1,2} \cos \theta_k \frac{\partial l_{Sk}(d, A_L)}{\partial d} \right], \quad (\text{S18})$$

which gives us the table of  $\nabla_d E_T(d, A_L)$  for each sample of  $(d, A_L)$ .

### S4 PRECONDITIONED TIME INTEGRATION OF HAIR

For the dynamics of elastic rods, we extend the work of Tournier et al. (2015) who proposed a stable and efficient constrained solver. We employ this solver since it is linear, stable at moderate time step, and is effective for constraints with a large range of stiffnesses.

In the following we first present our extended version of their method, which supports viscous drag and damping forces, and a novel preconditioner to boost the solver's efficiency for large systems with many inter-hair constraints.

We use  $\phi$  to denote the constraints on positions (for example  $\phi_{ij} = \|\mathbf{q}_i - \mathbf{q}_j\| - l_0$  for a spring with rest-length  $l_0$ ), where  $\mathbf{q}$  refers to the configuration (position).  $\dot{\phi}$  for viscous constraints on velocity, for example  $\phi_v = \dot{\mathbf{q}} - \dot{\mathbf{q}}_0$  for the drag force whose target velocity is  $\dot{\mathbf{q}}_0$ ;  $C$  for the diagonal positional compliance matrix, which is the inverted stiffness matrix for positional constraints; and  $C_v$  for

the diagonal viscous compliance matrix, which stores the inverted viscous drag coefficients.

The energy of positional constraints is

$$E = \frac{1}{2} \phi^T C^{-1} \phi, \quad (\text{S19})$$

and of viscous constraints is

$$E_v = \frac{1}{2} \dot{\phi}_v^T C_v^{-1} \dot{\phi}_v. \quad (\text{S20})$$

We denote the states at the next time step with a subscript "+". By linearization we have

$$\phi_+ \approx \phi + hJ\dot{\mathbf{q}} \quad (\text{S21})$$

where  $h$  is the time step and  $J := \frac{\partial \phi}{\partial \mathbf{q}}$ , and

$$\phi_{v,+} \approx \phi_v + hJ_{xv}\dot{\mathbf{q}}_+ + J_v(\dot{\mathbf{q}}_+ - \dot{\mathbf{q}}) \quad (\text{S22})$$

where  $J_{xv} := \frac{\partial \phi_v}{\partial \mathbf{q}}$  and  $J_v := \frac{\partial \phi_v}{\partial \dot{\mathbf{q}}}$ .

Since the constraint forces are conservative, they arise as the negative gradient of the corresponding potentials, giving the form

$$\begin{aligned} \mathbf{f}_c &= -\frac{\partial E}{\partial \mathbf{q}} = -\frac{\partial \phi}{\partial \mathbf{q}} \frac{\partial E}{\partial \phi} = J^T \lambda \\ \mathbf{f}_{cv} &= -\frac{\partial E_v}{\partial \dot{\mathbf{q}}} = -\frac{\partial \phi_v}{\partial \dot{\mathbf{q}}} \frac{\partial E_v}{\partial \phi_v} = J_v^T \lambda_v \end{aligned} \quad (\text{S23})$$

where  $\lambda$  and  $\lambda_v$  are the Lagrange multipliers of the positional and viscous constraints.

By the elastic constitutive law of the constraint forces (Lacoursiere 2007; Servin et al. 2006),  $C\lambda = -\phi$ , we have

$$\lambda_+ = -C^{-1}(\phi + hJ\dot{\mathbf{q}}_+) \quad (\text{S24})$$

and

$$\lambda_{v,+} = -C_v^{-1}[\phi_v + h(J_{xv} + h^{-1}J_v)\dot{\mathbf{q}}_+] + C_v^{-1}J_v\dot{\mathbf{q}}. \quad (\text{S25})$$

Then with linearized implicit Euler (Baraff and Witkin 1998) we have

$$(M - h^2K)\dot{\mathbf{q}}_+ = M\dot{\mathbf{q}} + h[\mathbf{f}_e - J^T C^{-1} \phi - J_v^T C_v^{-1}(\phi_v - J_v \dot{\mathbf{q}})] \quad (\text{S26})$$

where  $\mathbf{f}_e$  contains the constant external forces (gravity, etc.) and velocity impulses from fluid pressure (Section 4.3), and  $K = \frac{\partial(\mathbf{f}_c + \mathbf{f}_{cv})}{\partial \mathbf{q}} + \frac{\partial \mathbf{f}_{cv}}{\partial \dot{\mathbf{q}}}$  is the stiffness matrix.  $K$  can be re-formulated by substitution into the form

$$\begin{aligned} K &= - \underbrace{[J^T C^{-1} J + J_v^T C_v^{-1} (J_{xv} + h^{-1} J_v)]}_{\text{material stiffness}} + \\ &\quad \underbrace{\frac{\partial J^T}{\partial \mathbf{q}} : \lambda + \left( \frac{\partial J_v^T}{\partial \mathbf{q}} + h^{-1} \frac{\partial J_v^T}{\partial \dot{\mathbf{q}}} \right) : \lambda_v}_{\text{geometric stiffness}} \end{aligned} \quad (\text{S27})$$

where the notation ":" denotes the tensor product in the dimension of the number of constraints. The *material stiffness* terms represent the change of magnitude of constraint forces, while the *geometric stiffness* terms encode the transverse variation in force direction.

During each time step, we first compute  $K$  with (S27) using  $\lambda$  and  $\lambda_v$  computed from previous steps. We then solve (S26). After  $\dot{\mathbf{q}}_+$  is obtained, we update the Lagrange multipliers with (S24) and (S25).

*Remark.* For the adhesive/repulsive force of (20), we divide its intensity by the distance of the point-point pair to get the inverse compliance, where the material stiffness is then computed as

$$J_{ij}^T C_{ij}^{-1} J_{ij} = \hat{\mathbf{n}}_{ij} \frac{\|f_{s,ij}(d_{ij})\|}{d_{ij} - r_i - r_j} \hat{\mathbf{n}}_{ij}^T, \quad (\text{S28})$$

and similarly for the geometric stiffness.

As described in the main text, we precondition via local hair solutions. Recall that we partition the stiffness matrix into individual hairs and a cohesive term:

$$K\mathbf{x} = \sum_i^N K_i S_i \mathbf{x} + K_G \mathbf{x}. \quad (\text{S29})$$

Since each  $K_i$  only a few degree of freedoms are involved, and these smaller systems can be solved in parallel for all the hairs. Using the locally-solved velocity as an initial guess, we begin the preconditioned conjugate gradient method (PCG), using the local matrices  $M_i - h^2 K_i$  for preconditioning. Each local matrix is small, banded, and remains fixed between PCG iterations; it can therefore be easily factored at the beginning of the PCG loop, and solved in parallel with a fast banded solver (see Pseudocode S1).

In the pseudocode, we have denoted the left hand side of (S26) as  $A$ , the left hand side of (S26) considering only the constraints inside the  $i$ -th hair as  $A_i^*$ , the right hand side of (S26) as  $\mathbf{b}$ , and the right hand side of (S26) considering only the constraints inside the  $i$ -th hair as  $\mathbf{b}_i^*$ . We use the notation  $[\cdot]$  for the assembly of the local vectors into a global vector. Finally, we have defined the updated generalized velocities for a particular hair  $i$  via  $\dot{\mathbf{q}}_{+,i} := S_i \dot{\mathbf{q}}_+$ .

```

1: for all  $i$  do in parallel
2:   Solve  $A_i^* \dot{\mathbf{q}}_{+,i} = \mathbf{b}_i^*$ .
3: end for
4:  $\mathbf{r} \leftarrow \mathbf{b} - A[\dot{\mathbf{q}}_{+,i}]$ 
5: for all  $i$  do in parallel
6:   Solve  $A_i^* \mathbf{z}_i = S_i \mathbf{b}$ .
7: end for
8:  $\mathbf{z} \leftarrow [\mathbf{z}_i]$ 
9:  $\mathbf{p} \leftarrow \mathbf{z}$ 
10: while  $\mathbf{r}^T \mathbf{r} > \epsilon$  do
11:    $\mathbf{w} \leftarrow M \dot{\mathbf{q}}_+ - h^2 (\sum_i^N K_i S_i \dot{\mathbf{q}}_+ + K_G \dot{\mathbf{q}}_+)$ 
12:    $\gamma \leftarrow \mathbf{r}^T \mathbf{z}$ 
13:    $\alpha \leftarrow \frac{\mathbf{r}^T \mathbf{z}}{\mathbf{p}^T \mathbf{w}}$ 
14:    $\dot{\mathbf{q}}_+ \leftarrow \dot{\mathbf{q}}_+ + \alpha \mathbf{p}$ 
15:    $\mathbf{r} \leftarrow \mathbf{r} - \alpha \mathbf{w}$ 
16:   for all  $i$  do in parallel
17:     Solve  $A_i^* \mathbf{z}_i = S_i \mathbf{r}$ .
18:   end for
19:    $\mathbf{z} \leftarrow [\mathbf{z}_i]$ 
20:    $\beta \leftarrow \frac{\mathbf{z}^T \mathbf{r}}{\gamma}$ 
21:    $\mathbf{p} \leftarrow \mathbf{z} + \beta \mathbf{p}$ 
22: end while

```

Pseudocode S1. Locally-Preconditioned Solve

## S5 CROSS-HAIR LIQUID SIMULATION

As mentioned in §4.2, we simulate liquid flow not only along hairs (at smaller time scales) but across hairs (at slower time scales). Because

cross-hair liquid flow operates at a slow time scale, it may have a relatively less significant effect for many scenarios.

We begin with the potentially-connected vertex-hair pairs of the cohesion graph (recall Fig. 16 and §4.1.1), from which we construct vertex-vertex pairs: for each potentially-connected vertex-hair pair, we connect the source vertex to either of the two endpoints of the receiving edge, if the connection distance is within  $d_{\max}$ , thus producing up to two new vertex-vertex pairs.

Taking the union of all these vertex pairs and the vertices and edges of all the individual hairs generates a (typically multiple component) graph of all the connections between vertices along which liquid can flow.

We model flow along this graph as follows. Different from (13), in this case, the conservation law of mass is in 3D,

$$\frac{\partial H}{\partial t} + \nabla \cdot (Hu) = 0,$$

where  $H = (h + r)^2 - r^2$  is the local liquid thickness on hair.

We first compute the liquid velocity along the hair using (26) and perpendicular to the hair using (16). Similar to simulating reduced liquid along the hair, we store  $H_j$  at hair vertex  $j$ . Then, the conservation law of mass discretized in 3D becomes

$$(I + \delta t G) \mathbf{H}^{k+1} = \mathbf{H}^k,$$

where  $I$  is the identity operator, and

$$G = W_V^F d(\mathbf{u}^i) g_F - d^{-1}(l_j) g_F^T d(l^i) d^T(\mathbf{u}^i).$$

Here the notation are defined as follows:  $d(\mathbf{u}^i)$  is an operator that creates a block diagonal matrix using  $(\mathbf{u}^i)^T$  as its diagonal element.  $g$  is the finite different gradient operator over graph edges, and lastly  $W_V^F$  is the interpolation matrix that interpolate quantities defined at vertices using quantities defined on edges. We note the similarity of this approach to the earlier work of Azencot et al. (2015); our network approach can be viewed as a graph-theoretic analogy to their discrete surface based model.

## REFERENCES

- Omri Azencot, Orestis Vantzos, Max Wardetzky, Martin Rumpf, and Mirela Ben-Chen. 2015. Functional thin films on surfaces. In *Proceedings of the 14th ACM SIGGRAPH/Eurographics Symposium on Computer Animation*. ACM, 137–146.
- David Baraff and Andrew Witkin. 1998. Large steps in cloth simulation. In *Proceedings of the 25th Annual Conference on Computer Graphics and Interactive Techniques (SIGGRAPH '98)*. ACM, New York, NY, USA, 43–54. <https://doi.org/10.1145/280814.280821>
- Adhémar-Jean-Claude Barré de Saint-Venant. 1871. Théorie du mouvement non permanent des eaux, avec application aux crues des rivières et à l'introduction des marées dans leur lit. (1871), 11 p. Extrait des Comptes rendus de l'Académie des Sciences, tome LXXIII, séances des 17 et 24 juillet 1871.
- Ye Fan, Joshua Litven, David IW Levin, and Dinesh K Pai. 2013. Eulerian-on-lagrangian simulation. *ACM Transactions on Graphics (TOG)* 32, 3 (2013), 22.
- Claude Lacoursiere. 2007. Ghosts and machines: regularized variational methods for interactive simulations of multibodies with dry frictional contacts. (2007).
- Martin Servin, Claude Lacoursiere, and Niklas Melin. 2006. Interactive simulation of elastic deformable materials. In *Proceedings of SIGRAD Conference*. Linköping University Electronic Press.
- Maxime Tournier, Matthieu Nesme, Benjamin Gilles, and François Faure. 2015. Stable constrained dynamics. *ACM Transactions on Graphics (TOG)* 34, 4 (2015), 132.
- Thomas Young. 1805. An essay on the cohesion of fluids. *Phil. Trans. R. Soc. Lond.* 95 (1805), 65–87.

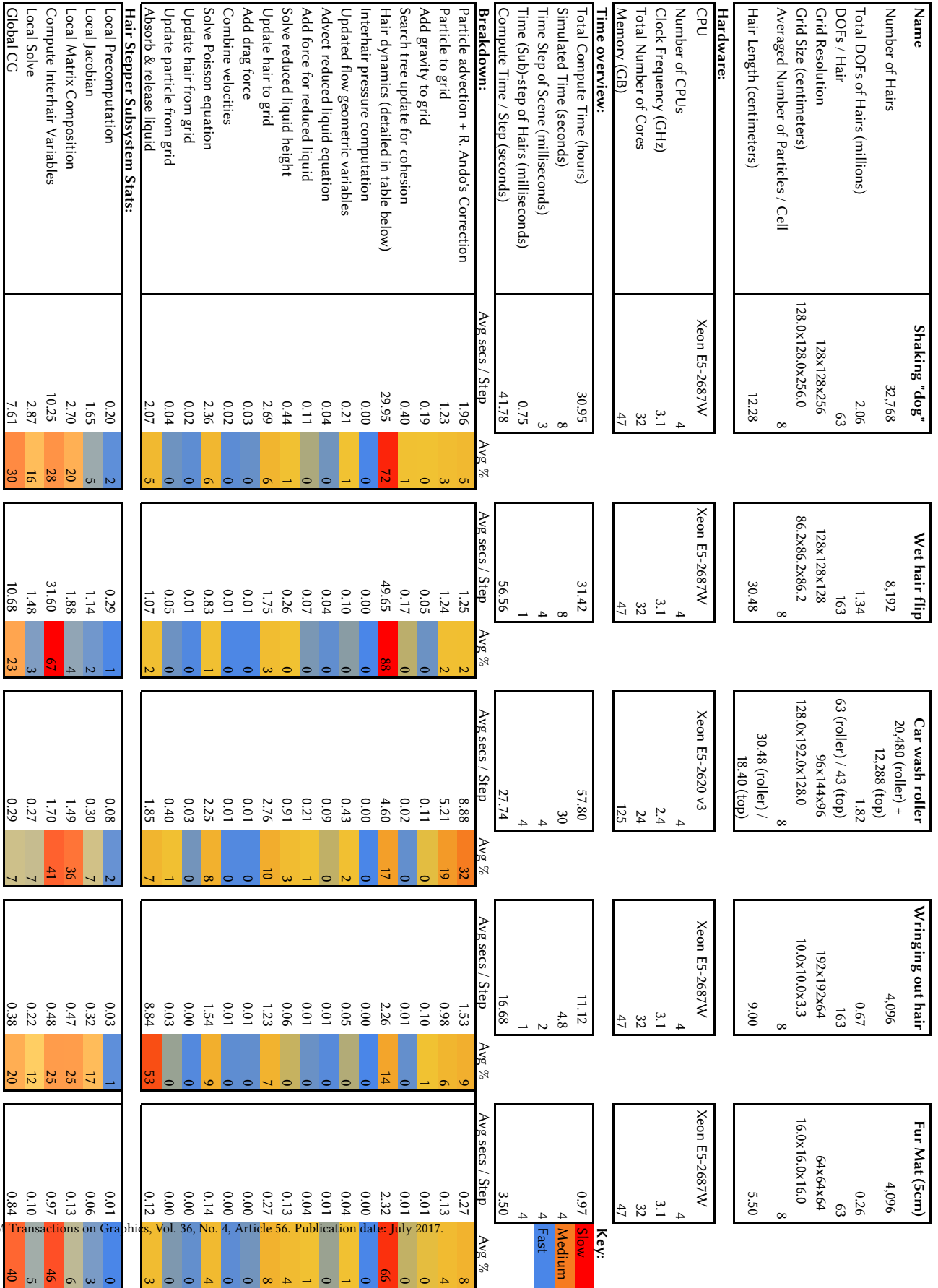


Fig. S1. Computational performance measurements.

## S6 NOTATIONS USED IN THIS PAPER

$\mathbf{d}$  differential operator  
 $\mathbf{ds}$  a small piece of hair segment  
 $E_s$  surface energy of liquid bridges  
 $\sigma$  surface tension coefficient of the liquid-air interface  
 $\theta$  equilibrium contact angle  
 $l_A$  arc length of the liquid-air boundary  
 $l_S$  arc length of the hair-air boundary  
 $\Omega_L$  the curve of a hair strand  
 $R$  the radius of the liquid bridge  
 $\alpha$  the angle between the liquid-air interface and the centerline of liquid bridge  
 $r$  the reciprocal of the mean curvature of the solid surface / the radius of hairs / the radius of capillarity  
 $A_L$  the cross-sectional area of the liquid region  
 $d$  the distance between two hair segments  
 $d_{\max}$  the maximal distance allowing the formation of liquid bridge  
 $k$  the stiffness of penalty force  
 $u$  the liquid velocity  
 $t$  the temporal variable  
 $p$  the liquid pressure  
 $a$  the external acceleration applied  
 $\rho_L$  the mass density of liquid  
 $h$  the liquid layer radius  
 $\mathbf{v}_{H_i}$  the  $i$ -th component of Lagrangian hair velocity  
 $\omega$  the angular velocity in the degree of freedom for hair twisting  
 $\nu$  the liquid viscosity  
 $\vartheta$  the angle between the hair strand direction and the direction of relative velocity of the hair and the surrounding bulk liquid.  
 $N$  the number of hairs  
 $d_{\perp}$  the perpendicular drag  
 $d_{\parallel}$  the longitudinal drag  
 $\phi$  the volume fraction of hairs  
 $w_{\text{FF}}$  the factor acts to smoothly disable the cohesion force if the quadrature pair lies beneath the bulk liquid surface  
 $m_{L,s,i,j}$  the liquid particle mass interpolated at averaged position of points  $i$  and  $j$   
 $\hat{m}_L$  a small positive threshold corresponding to average particle mass just beneath the free surface  
 $d_{\text{cell width}}$  the length of a grid cell  
 $l_{ij}$  the length of the source subdomain which contains point  $i$  and is connected with point  $j$   
 $E_{s,ij}$  surface energy of liquid bridges between quadrature pair  $i$  and  $j$   
 $K$  the stiffness matrix  
 $K_G$  the inter-hair coupling components  
 $S_i$  a diagonal *selection matrix* whose  $j$ -th term is one if the  $j$ -th degree of freedom belongs to the  $i$ -th hair and zero otherwise  
 $\mathbf{e}(x)$  centerline unit tangent at  $x$   
 $\{u^1, u^2, \dots, u^{M-1}\}$  edge-based coefficients in reduced flow  
 $\{h_1, h_2, \dots, h_M\}$  vertex-based coefficients in reduced flow  
 $l_i$  the length of edge  $i$   
 $l^i$  the vertex-based length for hair vertex  
 $\Delta t$  the time step size

$u^{j,(k)}$  the liquid velocity for edge  $j$  at time step  $k$   
 $\tilde{u}^{j,(k)}$  the backtraced liquid velocity for edge  $j$  at time step  $k$   
 $H_j^{(k)}$  the area of reduced liquid around a hair for vertex  $j$  at time step  $k$   
 $\langle \cdot \rangle_j^i$  the operator that converts edge-based quantities into vertex-based quantities  
 $m_{ai}^n$  the mass of liquid for grid node  $i$  in the  $a$  direction at time step  $n$   
 $u_{ai}^n$  the velocity of liquid for grid node  $i$  in the  $a$  direction at time step  $n$   
 $w_{aip}^n$  the trilinear interpolation weight that transfers the information on particle  $p$  to grid face  $i$  for direction  $a$   
 $\tilde{u}_{ai}^n$  the divergence-free velocity for grid node  $i$  in the  $a$  direction at time step  $n$   
 $\mathbf{c}_{pa}^n$  the vector introduced for the purpose of preserving the affine velocity field  
 $\rho_H$  the mass density of hair  
 $m_h$  the mass of a hair vertex including its reduced-liquid  
 $D_{ai}^n$  the averaged drag force for grid node  $i$  in the  $a$  direction at time step  $n$   
 $M_{ai}^n$  the reduced-liquid masses for grid node  $i$  in the  $a$  direction at time step  $n$   
 $T_{ai}^n$  the momentum contributed from the reduced-liquid for grid node  $i$  in the  $a$  direction at time step  $n$   
 $\mathbf{v}_H^n$  the Lagrangian hair velocity at time step  $n$   
 $V_{H_i}^n$  the volume of hair vertex  $i$  at time step  $n$   
 $V_{L_i}^n$  the volume of reduced liquid around hair vertex  $i$  at time step  $n$   
 $V_i^n$  the volume of bulk liquid for particle  $i$  at time step  $n$   
 $I$  the identity matrix